Generalized competition interfaces for TASEP

C. Cioli[1]

[1]*Center for Complexity Science, University of Warwick, Coventry CV4 7AL, UK*

(Dated: August 31, 2011)

Competition interfaces have been studied recently in a number of papers for particular simplified solid on solid growth model in connection with totally asymmetric exclusion process (TASEP). For a particular rule of type propagation the competition interface is related to the location of a second class particle, which has been studied extensively and is well understood. In this paper, we investigate several natural generalizations of the type propagation, which can also be studied in the context of special particles in the TASEP different from second class particles. A mathematically rigorous description turns out to be rather challenging.

PACS numbers:

I. INTRODUCTION

The capability to model a competing interface between two different growing media is a topic of high relevance. This turns out to be the very basic step towards the understanding of many heterogeneous complex systems studied in different disciplines as physics, chemistry and biology [1–7]. To understand the dynamics and the statistics of such surfaces is in fact relevant to have an insight in segregation phenomena, clusters evolution, phase transition that can be encountered in systems like liquid crystals, growing bacteria colonies, growing crystals, spin systems [7–11]. Of fundamental importance are in these cases inheritance rules which play the role of driving force in shaping competing interfaces.

Recently the study of competition interfaces using simplified models related to TASEP (totally asymmetric simple exclusion process) processes has become a central issue. One dimensional TASEP has been widely exploited to model growing surfaces belonging to 1+1 universality class of KPZ and in the last few years, particularly in connection with the solid on solid growth model [12–17]. In this model while particles (called also first class particles) in the TASEP lattice jump right with rate one towards neighbouring empty sites, each successful jump determines the birth of one new brick on the surface in such a way that each brick has two parents.

A so-called second class particle follows the same rules of a first class one, but can be overtaken by the other particles. It has been shown [14–16] that the dynamics of the horizontal coordinate of a competition interface is given by the location of a second class particle in the TASEP, which is directly related to last-passage percolation [18, 19]. This connection comes from the inheritance law determining the dynamics: the new individual always inherits the type of the younger parent. Last-passage percolation roughly consists of finding a path of maximal weight in a given random environment and is strictly connected with directed polymer theory [17]. The study of this class of simplified models has led to a very detailed understanding of asymptotic properties such as speed or fluctuations [14] characterizing second class particle but the rule it follows turns out to be quite strict when trying to reproduce the inherent and total stochasticity showed by real complex systems (e.g: biological context of species segregation [7, 8]). It is then interesting to study and to understand the dynamics and the statistics owned by competing interfaces resulting from different inheritance laws. This leads to introduce a new type of particle in the TASEP context which has not been studied so far, named sector particle. In the following we focus first on stationary initial conditions, a thorough understanding of which is a first step to understand more general ones such as cones [18].

This work is organized as follows: in Section II we present the connection between solid on solid growth model and TASEP model and we summarize the main features about second class particle in relation with competing interfaces; in Section III we firstly explain our simulation choices, we then display results about second class particle to test the validity of our numerical tools; we finally show numerical results obtained for sector particle and two different attempts to explain analytically the behaviour of that; in Section VI we discuss further results for sector/second class particle simulated using deterministic initial conditions and we briefly present numerical data about several different generalizations of the two extreme cases of second class particle and sector particle. Sec.V is devoted to conclusions and perspectives.

II. THEORETICAL BACKGROUND

A. TASEP and solid on solid growth model

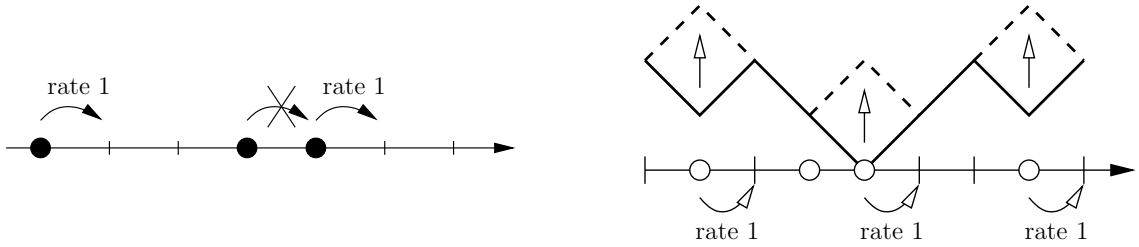

FIG. 1: (Taken from [14]) TASEP and connection with solid on solid growth model (right panel: the surface above the tasep should be shifted 1/2 lattice site to the right to be consistent with our notation)

The TASEP is a continuous-time ergodic Markov chain, where identical particles jump to the right with rate one subject to an exclusion interaction (at most one particle per site) (see left panel of FIG. 1).

In this work we consider the TASEP on the integer lattice $\mathbb{Z}$ with state space $X = \{0,1\}^{\mathbb{Z}}$. The dynamics is defined by the generator

$$\mathcal{L}f(\eta) = \sum_{x\in\mathbb{Z}} \eta_x(1-\eta_{x+1})\big(f(\eta^{x,x+1}) - f(\eta)\big) \,, \tag{1}$$

where $\eta^{x,x+1}$ is the configuration where one particle was moved from x to $x+1$, i.e. $\eta_y^{x,x+1} = \eta_y - \delta_{x,y} + \delta_{x+1,y}$ for all $y \in \mathbb{Z}$. $\mathcal{L}$ is defined for suitable cylinder test functions $f : X \to \mathbb{R}$, for a full discussion about domains and the connection to Markov semigroups see the standard reference [24]. It is well known that this process has a family of stationary product measures ν_ρ with density $\rho \in [0,1]$ corresponding to the average number of particles per site.

The dynamics of the TASEP can be coupled to the evolution of a solid on solid surface growth model [22, 23] on the dual of the TASEP lattice. Let $h(y,t) \in \mathbb{Z}$ be the height of the surface for $y \in \mathbb{Z} + 1/2$, and the height gradient is restricted to ± 1 and connected to the TASEP configuration $\eta(t)$ via

$$h(x+1/2,t) - h(x-1/2,t) = 1 - 2\eta_x(t) \in \{-1,1\} \,. \tag{2}$$

The total height of the surface is not fixed, and one can arbitrarily take $h(1/2,0) = 0$ to fix an initial height profile for a given $\eta(0)$. A jump of a TASEP particle across the bond $(x, x+1)$ corresponds to the increase of the height $h(x+1/2,t)$ by one or the addition of a diagonal square brick (see right panel of FIG. 1). A stationary TASEP configuration with density $\rho \in [0,1]$ therefore corresponds to a tilted surface with angle $\alpha \in [-\pi/4, \pi/4]$ against the horizontal and $\tan\alpha = 1 - 2\rho$. It is well known that the surface $h(x,t)$ for this model belongs to the KPZ universality class [23] and undergoes kinetic roughening with exponent $1/3$ [10]. The macroscopic equation that governs the time evolution of height gradients is the Burgers equation for the density of particles in the TASEP

$$\partial_\tau \rho(u,\tau) + \partial_u j(\rho(u,\tau)) = 0 \,. \tag{3}$$

This reflects the conservation of mass in the TASEP, and can be derived rigorously in a scaling limit $\epsilon \to 0$ with $x = u/\epsilon$, $t = \tau/\epsilon$ [22]. Here $j(\rho) = \rho(1-\rho)$ is the stationary average current of the TASEP under distribution ν_ρ.

It is clear from the dynamics that a brick at site $x + 1/2$ can only be added if $\eta_x(t) = 1$ and $\eta_{x+1}(t) = 0$, i.e. $h(x-1/2,t) = h(x+3/2,t)$ and the new brick has two 'parent bricks' at $x - 1/2$ and $x + 3/2$.

B. Second class particle

As mentioned before when two different media are growing competing with each other the competing interface can grow according to different laws of inheritance. In the well studied case corresponding to last passage

percolation growth model, each time a brick has to be grown in correspondence of the competing surface, the brick type will be assigned based on the type of the younger parent. This evolution if mapped onto a TASEP lattice corresponds to the evolution of a so called second class particle.

The ancestry of a brick at the surface at time t corresponds to a (downward) directed path on the dual lattice $(\mathbb{Z}+1/2)^2$, that connects its type to the original ancestor at time 0. The set of all such paths forms a family of (upward directed) spanning trees on the set of all occupied bricks up to time t. A competition interface is then an upward directed path on $\mathbb{Z}^2$ dual to the ancestral trees, and the set of all such paths form a family of (downward directed) spanning trees of the grown part of $\mathbb{Z}^2$. Competition interfaces and ancestral lines are statistically equivalent under time reversal, which has been shown in [18]. In a TASEP context we describe the location of a second class particle by a hole-particle pair [14]. Its position can change in two ways: it can move one step forward with rate 1 to an empty site, and it can jump backward one step with rate 1 when a first class particle jumps over it (occupies the hole). The two cases are pictured below

$$..\boxed{01}0..\to..0\boxed{01}.. \quad \text{or} \quad ..1\boxed{01}..\to..\boxed{01}1.. \tag{4}$$

If the initial configuration of the lattice $\eta(0)$ is distributed according to the Bernoulli product measure ν_ρ with density ρ for all the sites $j < L/2$ and product measure ρ_λ with density λ for all the sites $j > L/2$ then for the position of the second class particle X_t is shown that [14–16]

$$\lim_{t\to\infty}\frac{X_t}{t}=\begin{cases}1-\rho-\lambda & \text{if } \lambda\le\rho\\ U & \text{if } \lambda>\rho\end{cases} \tag{5}$$

and for the inclination of the competing interface

$$\tan\alpha=\begin{cases}\frac{\lambda\rho}{(1-\lambda)(1-\rho)} & \text{if } \lambda\le\rho\\ \frac{1-U}{1+U}^2 & \text{if } \lambda>\rho\end{cases} \tag{6}$$

where U is a random variable uniformly distributed in $[1-2\rho, 1-2\lambda]$ and the angle $\alpha\in[0,90^o]$.

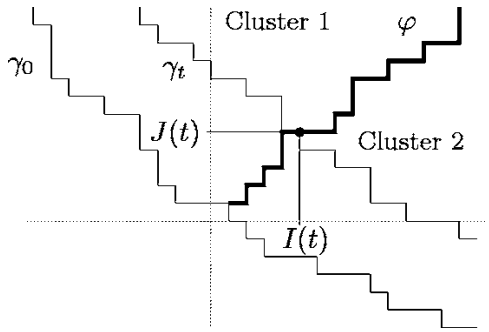

FIG. 2: (Taken from [14]) Second class particle and competition interface: γ_0 is the initial profile of the growing surface, γ_t represent the growing surface at time t; ϕ is the competing interface between clusters 1 and 2, while $(I(t), J(t))$ is the position of the second class particle at time t.

C. Generalization of the second class particle framework

As mentioned in the introduction the rule followed by a second class particle turns out to be too strict if we are aiming to describe completely stochastic real systems. In this work, we will then study the rules reported below and compare them, including second class one for completeness. The initial configuration $\eta(0)$ of the TASEP lattice will distributed according to the Bernoulli product measure ν_ρ with density ρ for all L the sites, unless it is stated differently.

- Let X_t be the interface generated by inheriting the type from the younger parent, it is known that $X_t/t \to v_X(\rho) = j'(\rho) = 1-2\rho$ and $Var(X_t) = (X_t - tv_X(\rho))^2 \sim t^{4/3}$. The fluctuations are also expected to be non-Gaussian with heavier tails.
- Let Y_t be the interface generated by inheriting the type from the older parent. The simulations suggest that we have a law of large numbers for the speed $Y_t/t \to v_Y(\rho)$, and the fluctuations are of order t and Gaussian.

- Let Z_t^q be the interface generated by inheriting the type from the older parent with probability q, otherwise the younger parent. This interpolates between X_t and Y_t, and for $q = 1/2$ it is easy to see that the interface performs a random walk without drift, i.e. $Z_t/t \to v_Z(\rho) = 0$ for all $\rho \in [0, 1]$. Fluctuations asymptotic behaviour turns out to be of order t with the same features displayed by a sector particle for $q < 0.5$; to behave like t for all t in the case of $q = 0.5$ since the particle/competing surface is performing a pure brownian motion; to have different asymptotic behaviours (proportional to t or $t^{4/3}$) depending on ρ for $q > 0.5$.

Analogous to scheme 4 for the second class particle location X_t [14], we will describe the location of a sector particle Y_t by a hole-particle pair. This can change in two ways, the particle can hop forward or the hole backward (i.e. another particle jumps on hole). Whereas X_t immediately moves forward or backward following the first event (yielding a new hole-particle pair by construction), Y_t only moves after both, the particle and the hole have jumped, and it follows the second one. Thereby it undergoes an intermediate state 00 which results in an ultimate left move, or 11 resulting in a right move. In short

$$..\boxed{01}..\to ..\boxed{00}1.\to .\boxed{01}0.. \quad \text{or} \quad ..\boxed{01}..\to .0\boxed{11}..\to ..1\boxed{01}. \tag{7}$$

where in the second transition the location of Y_t marked by the box jumps to the left or right, and the dots denote sites which are not determined after a jump.

III. NUMERICAL ANALYSIS

A. Simulation method

Our simulation results are obtained in a TASEP on the lattice $\mathbb{Z}/L\mathbb{Z}$ with periodic boundary conditions and typically $L = 1024$. The initial configuration $\eta(0)$ is distributed according to a single Bernoulli product measure ν_ρ so that we are in the case $\lambda = \rho$ of Eq. 5. This kind of initial conditions are called stationary initial conditions: fixed ρ, $n = \rho L$ particles are positioned picking sites at random till each particle has been set; the initial position of the special particles (second class or sector) X_0 or Y_0 is set to be equal to 0. The surface is periodically extended at the boundaries, which leads to finite size effects when the lateral correlation lengths reach the size of the system. This effect can be seen in the fluctuations behaviour for X_t, which turns out to be asymptotically proportional to t rather than $t^{4/3}$. The t behaviour is visible for early t as well. This phenomenon is also due to finite size effects, as proved running some simulations for different system sizes (L=512, 1024, 2000, 4000) and comparing the rescaled fluctuations for two different values of ρ ($\rho = 0.1, 0.5$) (FIG. 5). The system is typically evolved for a time $t_{max} = 100L$ and the ensemble used to average on, ranges from 100 to 4000 repetitions of the experiment according to the eventual need to evaluate properly PDF tails. This because eventual features of interest can be found on tails as for example in the case of second class particle: tails are in fact expected to be non-Gaussian due to this particle dynamics to belong to KPZ universality class.

The TASEP processes are simulated using a Monte Carlo algorithm based on random sequential update, which corresponds to the simulation of the jump chain of the Markov model. At each time step, one non empty lattice site i is chosen uniformly at random from the $n = \rho L$ non empty sites and two operations are performed

- Attempt to update selected first class particle position: if the right neighbour site j is empty the particle jumps to the right and the current counter is raised of one unit
- Check if i or $i + 1$ corresponds to the hole or the particle of a second class/sector particle in their box representation (ref); in which case the particle position is non/updated based on their dynamics rules 4 and 7

Since the system behaviour is symmetric about $\rho = 0.5$ and so is the second class and sector particles dynamics, the choice of picking at random a non empty site instead of one of the L lattice sites has been made observing that using values of $\rho \in [0, 0.5]$ results to be computationally more efficient. This is easy to understand if we take into account that the selection of an empty site does not lead to an update of the system configuration. From this follows that the time counter $t \to t + Exp(n)$ is updated by adding an exponential random variable with mean $1/n$ which is the waiting time of the Markov chain.

B. Analysys of X_t

As mentioned above second class particle dynamics is well known and studied in literature. In this section are summarized the main numerical results about this particle behaviour in order to show the validity of our analysis

tools and to easily compare results obtained for sector particle and all intermediate cases presented in Sec. IV; the dynamics of intermediate cases results in fact from the mixing of the second class and sector particle behaviour. Initial conditions used are as specified before stationary initial conditions distributed according to a single Bernoulli product measure ν_ρ with density ρ on the overall extension of the lattice: we then expect the second class particle to follow a characteristic and to move with speed (from Eq. 5 and Eq. 6)

$$v_X = \lim_{t\to\infty} \frac{X_t}{t} = 1 - 2\rho \tag{8}$$

Fluctuations $Var(X_t) = (X_t - tv_X(\rho))^2$ are expected to show a behaviour proportional to $t^{4/3}$ [17] till time $t = \beta L^{3/2}$ where β is a prefactor depending on ρ and dictated by correlations among particles positions. In FIG. 3 are compared numerical data produced for the asymptotic speed and fluctuations for a second class particle with the analytical forecast. The agreement between the two results to be verified (regarding speed data, error bars are smaller or equal to markers size); in FIG. 4 is stressed and made clearer the presence of the two different regimes $t^{4/3}$ for $t \leq \beta L$ and t due to finite size effects. FIG. 4 is also highlighting a peculiar behaviour for the fluctuations at early time: this seems to be proportional again to t for some values of ρ. This phenomenon is not reported in literature; it turns out to be not an artifact of our simulation methods but as demonstrated in FIG.4 is again due to finite size effect: these plots show the rescaled fluctuations respectively for $\rho = 0.1$ and $\rho = 0.5$ and for different system sizes (L=512,1024, 2000, 4000). The early time behaviour not proportional to $t^{4/3}$ is clearly fading out as the system size increases. $X_t - v_X t$ is further known to show Gaussian PDF with heavy tails not belonging to Brownian motion universality class. Rescaled numerical data for $PDF(X_t - v_X t)$ behave as expected if analysed for t falling in the $t^{4/3}$ regime.

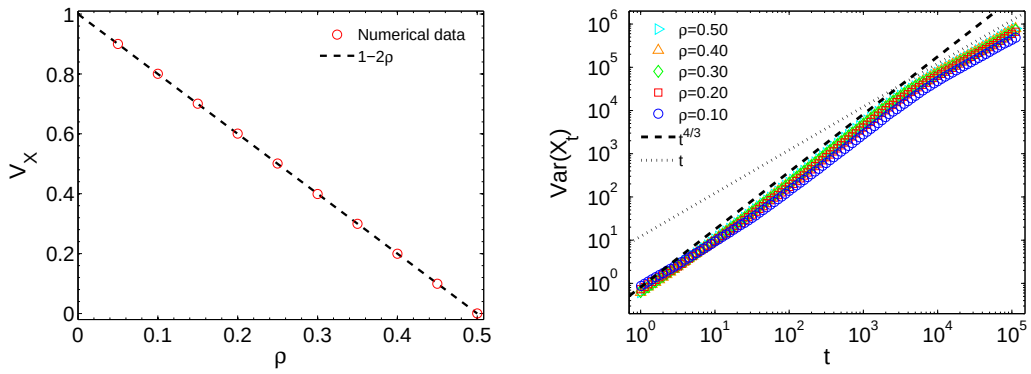

FIG. 3: Comparison between numerical and analytical data: asymptotic velocity (Eq. 8: $v_X = 1 - 2\rho$) of a second class particle as a function of ρ (left panel); simulated fluctuations for a second class particle (right panel). Data points are obtained on a lattice with L=1024; for each value of ρ, simulations for X_t evolution are repeated 4000 times, each for a time $t_{max} = 100L$.

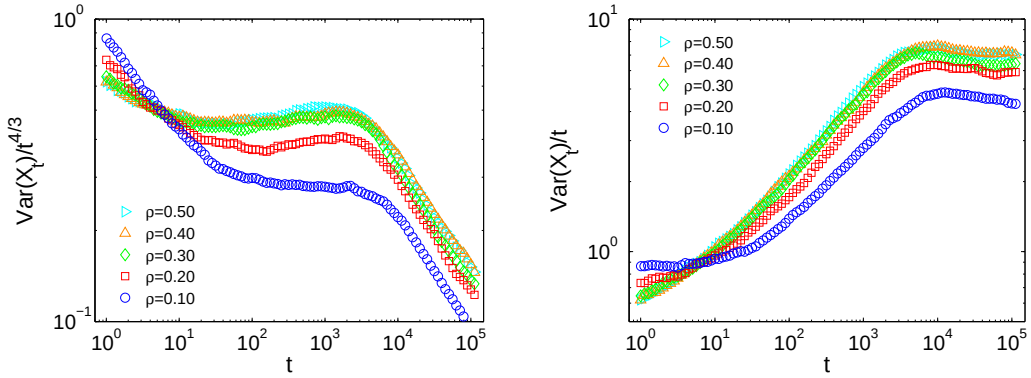

FIG. 4: Time rescaled fluctuations for a second class particle:t regime (left panel) $t^{4/3}$ regime (right panel). Data points are obtained on a lattice with L=1024; for each value of ρ, simulations for X_t evolution are repeated 4000 times, each for a time $t_{max} = 100L$.

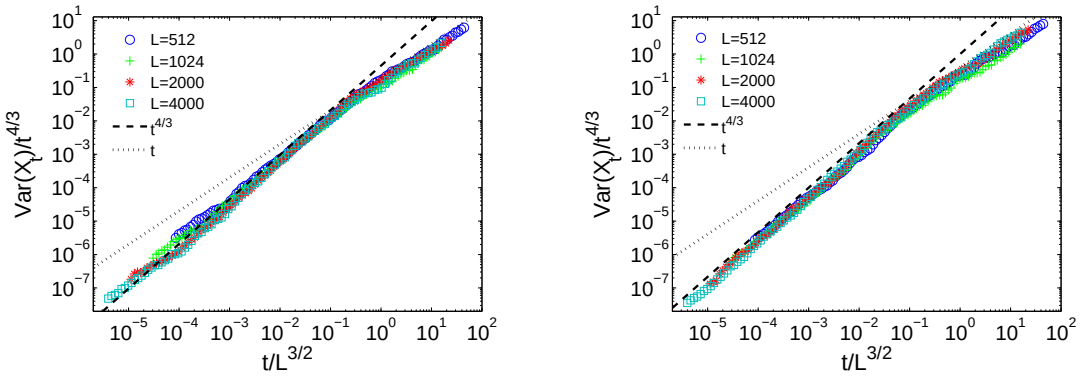

FIG. 5: Rescaled fluctuations for several system sizes ($L = 512, 1024, 2000, 4000$): $\rho = 0.1$ (left panel) $\rho = 0.5$ (right panel). Data points are obtained on lattices with L=512, 1024, 2000, 4000; for each value of L and ρ, simulations for X_t evolution are repeated 100 times, each for a time $t_{max} = 100L$.

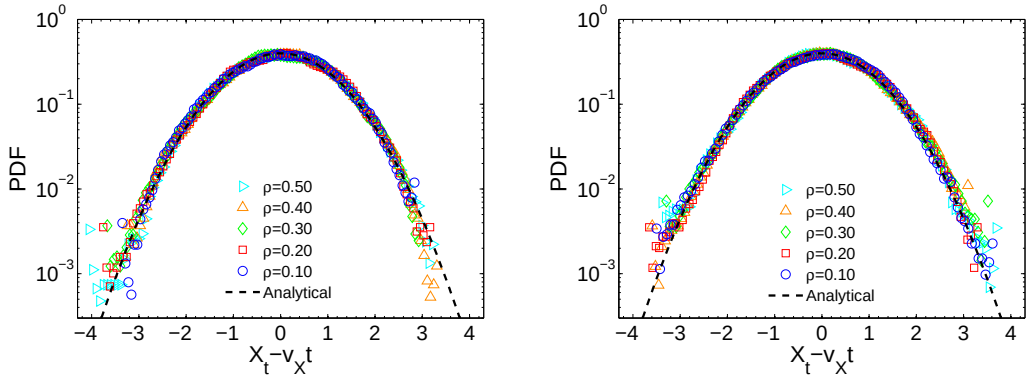

FIG. 6: PDF for $X_t - v_X t$ evaluated for time $t = 10L$ (left panel) and $t = 100L$ (right panel) in correspondence of the $t^{4/3}$ regime. Data points are obtained on a lattice with L=1024; for each value of ρ, simulations for X_t evolution are repeated 4000 times, each for a time $t_{max} = 100L$.

C. Analysis of Y_t

In this section are presented numerical data used to have a first insight about asymptotic speed and fluctuations displayed by Y_t indicating the displacement in function of time for the particle we have introduced, namely the sector particle. In FIG. 7 is shown the asymptotic speed (dots in black) for $\rho \in [0, 0.5]$ and this is compared with analytical curves derived as attempts to explain theoretically the asymptotic speed behaviour; the ideas behind are reported in the following subsections.

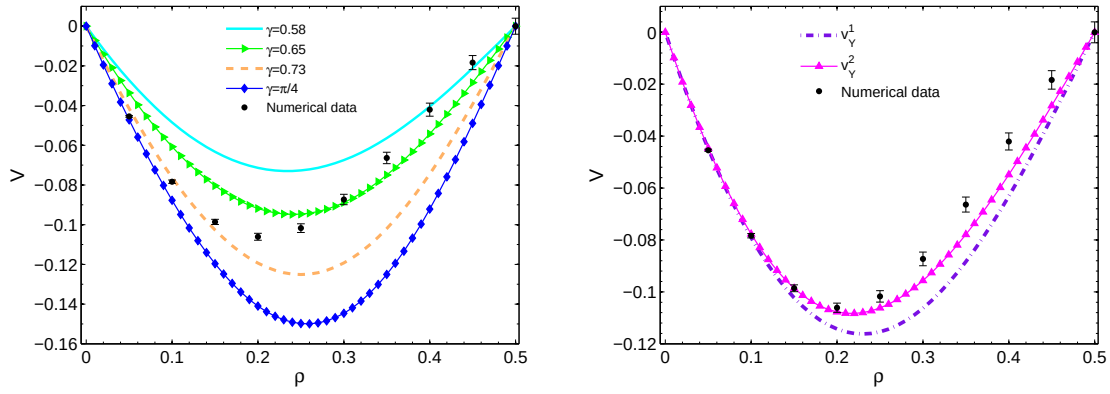

FIG. 7: Asymptotic speed for a sector particle: comparison against several trial analytical curves. Left panel: the analytical form are the one of Eq. 13, 11; right panel: 16, 21. Data points are obtained on a lattice with L=1024; for each value of ρ, simulations for v_Y evolution are repeated 4000 times, each for a time $t_{max} = 100L$.

1. *Speed parallel to lattice dimension and bricks geometry*

Our first attempt to find an analytical expression for the sector particle asymptotic speed v_Y , is to check if this speed is equivalent to the horizontal component of the overall growing surface speed: it is then necessary to evaluate the component of the growing surface speed parallel to the lattice dimension. The growth rate of the surface is given by

$$G = AjL \tag{9}$$

where j is the current, A is the area of a single brick; in the usual case $A = 2$ being bricks squares such that their emidiagonal is $h = 1$. The component perpendicular to the surface of its growing speed is then

$$v_{\perp}^{\frac{\pi}{4}} = \frac{G\cos\alpha}{L} = Aj\cos\alpha = A\rho(1-\rho)\cos\alpha \tag{10}$$

and using trigonometric calculus we obtain for the component parallel to lattice dimension

$$v_Y^{\frac{\pi}{4}}(\rho) = v_{\perp}\sin\alpha = 2\frac{(2\rho-1)\rho(1-\rho)}{1+(1-2\rho)^2} \tag{11}$$

where $\tan\alpha = 1 - 2\rho$ (see Sec. II Subsec. A)

The comparison between numerical and analytical curves is showed in FIG. 7 and turns out to be wrong. Nevertheless the two curves have similar characteristics as sign, concavity and symmetry. This lead us to investigate more deeply the features of solid on solid model used to mimic the growth of the surface. As mentioned previously the bricks used to model the growing surface are square bricks and these bricks have the property of having the emidiagonal $h = 1$. To save our hypothesis of a sector particle moving parallel to the lattice dimension we think to change the geometry of the bricks: maintaining the rhomboidal shape with emidiagonal $h = 1$, we introduce the parameter γ as the opening angle of the characteristic brick. It implies that the growth rate for the surface is now different and the tilt angle for it is given by

$$\tan\alpha = (1-2\rho)\tan\gamma \tag{12}$$

after some simple calculations we obtain

$$v_Y^\gamma(\rho) = 2\frac{(2\rho-1)\rho(1-\rho)\tan^2\gamma}{1+(1-2\rho)^2\tan^2\gamma} \tag{13}$$

The comparison between numerical and analytical data turns out to be still unsatisfactory: in FIG. 7 are pictured analytical curves for three different values of γ chosen as the one fitting the maximum number of numerical data. This approach leads to a weak agreement just ρ values close to $\rho = 0$ and $\rho = 0.5$ but for any value of γ fails to predict the numerical points for intermediate values of ρ.

2. *Local stochastic analysis*

In this subsection we try to model analytically Y_t by referring directly to the dynamics of the hole-particle pair as we described in 7 and that we show again below

$$..\boxed{01}..\to ..\boxed{00}1.\to .\boxed{01}0.. \quad \text{or} \quad ..\boxed{01}..\to .0\boxed{11}..\to ..1\boxed{01}. \tag{14}$$

We remember that dots denote sites which are not determined after a jump; if we integrate over these undetermined sites w.r.t. the stationary measure ν_ρ leads to a first (naive) guess of the speed of Y_t. The time it takes to make the transition is given by

$$T = \max\left\{Exp(\rho), Exp(1-\rho)\right\} \tag{15}$$

where $Exp(\rho)$ and $Exp(1-\rho)$ are the (independent) jump times of the hole and the particle. A simple computation yields that $\mathbb{E}(T) = \big(\rho(1-\rho)\big)^{-1} - 1$. Since the hole and the particle jump according to independent Poisson processes with rates ρ and $1-\rho$, respectively, the probability that the hole jumps first is ρ, and $1-\rho$ for the particle. Since Y_t follows only the second jump this leads to an average displacement of $2\rho - 1$ after one jump and therefore to the estimate

$$v_Y^1(\rho) = (2\rho-1)/\mathbb{E}(T) = \frac{(2\rho-1)\rho(1-\rho)}{1-\rho(1-\rho)}\,. \tag{16}$$

Comparing with the simulation we see that this is not accurate, in particular for densities close to $\rho = 0.5$. The reason for that are the correlations introduced through the situations after a jump as given in 7. This is in principle also the case for the second class particle X_t, but for Y_t the situation is worse. Due to total asymmetry of the hopping the empty site ahead (or the occupied behind) cannot be filled by another particle (or hole) before Y_t moves again. This introduces correlations for Y_t which turn out to be not present for X_t, since in that case there is either a particle ahead or a hole behind which are both free to move independently. Indeed it can be shown rigorously that the simple argument above gives the right speed for X_t, while our simulation results imply that for Y_t the correlations have to be taken into account.

A first simple approach to do this is to keep track of the last jump direction of Y_t. As can be seen in (7), after a left (right) jump there is a hole in front of (particle behind) Y_t, which makes it more likely that the next jump is again to the left (right). Assuming that all other sites are distributed independently according to ν_ρ, the jump times T_L, T_R after a left and right jump are given now by

$$T_L = \max\left\{Exp(\rho), Exp(1)\right\} \quad \text{and} \quad T_R = \max\left\{Exp(1), Exp(1-\rho)\right\} \tag{17}$$

which leads to expected values

$$\mathbb{E}T_L = 1 + \frac{1}{\rho} - \frac{1}{1+\rho} \quad \text{and} \quad \mathbb{E}T_R = 1 + \frac{1}{1-\rho} - \frac{1}{2-\rho}\,. \tag{18}$$

Furthermore, if we write p_{LR} for the probability that a left jump is followed by a right jump, we can compute all these probabilities with the Poisson process argument analogous to the above. This yields

$$p_{LL} = \frac{1}{1+\rho}\,, \quad p_{LR} = \frac{\rho}{1+\rho}\,, \quad p_{RL} = \frac{1-\rho}{2-\rho} \quad \text{and} \quad p_{RR} = \frac{1}{2-\rho}\,. \tag{19}$$

Considering this as a two-state Markov chain we find that it has the stationary distribution

$$q_R = \frac{\rho(2-\rho)}{1+2(1-\rho)\rho} \quad \text{and} \quad q_L = 1 - q_R = \frac{1-\rho^2}{1+2(1-\rho)\rho}\,, \tag{20}$$

which gives an estimate for the average fraction of right and left jumps of X_t for large t. This leads to a second estimate for the asymptotic speed

$$v_Y^2(\rho) = \frac{q_R - q_L}{q_R \mathbb{E}(T_R) + q_L \mathbb{E}(T_L)} = \frac{(2\rho - 1)\rho(1-\rho)}{1 - \rho(1-\rho)(1 - 2\rho(1-\rho))} \,. \tag{21}$$

As can be seen in the figure this is a better approximation than v_Y^1, but still slightly off for ρ close to 0.5. But taking into account higher order correlations than the one-step transitions in directions becomes very complicated, since they depend on the behaviour of the rest of the system.

Assuming that the variance is not influenced by the time, we get that it is proportional to t and

$$Var(Y_t) = < (Y_t^2)^2 > - (v_Y^2 t)^2 \tag{22}$$

where

$$< (Y_t^2)^2 > = t \, \frac{q_R + q_L}{q_R \mathbb{E}(T_R) + q_L \mathbb{E}(T_L)} = t \, \frac{\rho(1 + \rho(1 - 2\rho(2 - \rho)))}{1 - \rho(1-\rho)(1 - 2\rho(1-\rho))} \tag{23}$$

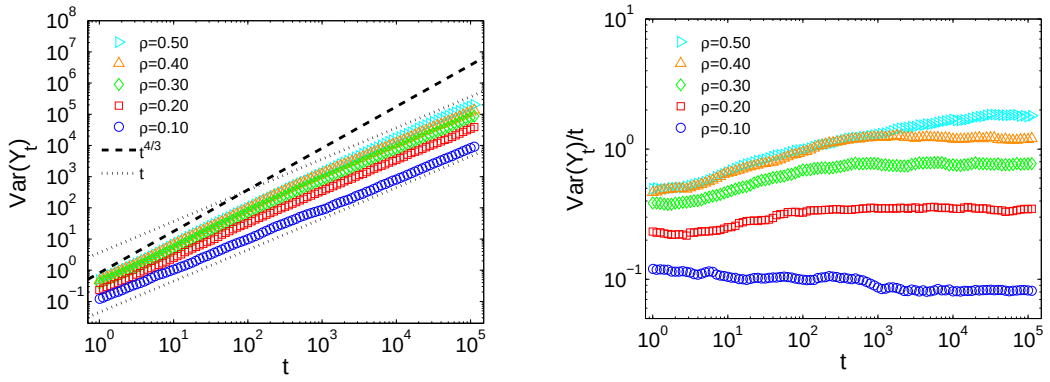

FIG. 8: Fluctuation for a sector particle (left panel); t rescaled fluctuations (right panel). Data points are obtained on a lattice with L=1024; for each value of ρ, simulations for Y_t evolution are repeated 4000 times, each for a time $t_{max} = 100L$.

Observing the right panel of FIG. 8 can be seen as fluctuations behaviour proportional to t is of course ρ dependent via the prefactor changing with ρ values but also time dependent. In FIG. 9this phenomenon is stressed. The analytical curve dashed in black is the analytical solution obtained taking in account first order correlations that drive the dynamics of the system (Eq. 22): for early time the curve well fits the numerical data, while for later time numerical data depart from this solution due to correlations arising in the system and not incorporated in the theoretical derivation. As clear in the right panel of FIG. 8 dependence of $Var(Y_t)$ with time ends after a time of order L^2. Fluctuations do not show then the typical behaviour proportional to $t^{4/3}$ displayed instead by second class particle but an asymptotically diffusive and time independent one while superdiffusive behaviour is displayed for early times. Another difference is clear from second class particle fluctuations: while for the latter for different values of ρ fluctuations points look shrinked spanning less than one orders of magnitude, in the sector particle case they turn out to be spreaded in function of ρ spanning almost two order of magnitude. Since the interfaces Y_t do not follow a characteristic in the system, its fluctuations are expected to be dominated by the fluctuations of the initial conditions of the population height and since we start with stationary initial conditions ν_ρ for the TASEP, these are expected to be dominated by the usual CLT, i.e. Gaussian with variance of order t. The behaviour proportional to t has been discussed before; the study of PDF for $Y_t - v_Y t$ leads to conclude reasonably that fluctuations own a Gaussian distribution at list asymptotically. It is clear following the evolution as time grows of the renormalized PDF ($Y_t - v_Y t$) in FIG. 10: while for early time $t = 0.1L$ (first panel) and $t = 10L$ (second panel) distributions display non-Gaussian tails being in the regime for which fluctuations show a strongly time dependent and superdiffusive behaviour (subdiffusive for $\rho \leq 0.1$), for $t = 100L$ where for each value of ρ fluctuations are proportional to t in a nearly time independent way (we approach $t \sim L^2$), tails start to lay on the analytical normalized Gaussian curve. Referring to first panel of FIG. 10, the asymmetry in the distribution for $t = 0.1L$ and for small densities is caused by asymmetric trajectories performed by sector particle. Due to geometric constraints of a largely tilted surface it can do only isolated jumps to the right, separated by several consecutive jumps to the left.

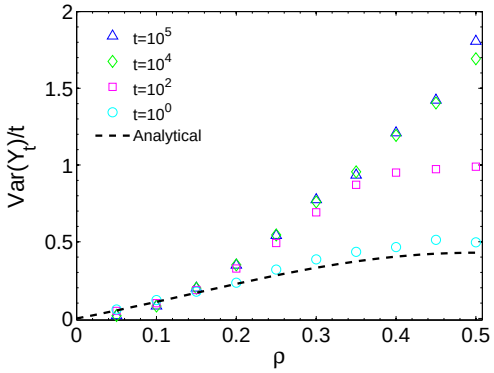

FIG. 9: Fluctuations at fixed times: correlations arising in the system make numerical data diverge from first order correlation analytical trial (Eq. 22). Data points are obtained on a lattice with L=1024; for each value of ρ, simulations for Y_t evolution are repeated 4000 times, each for a time $t_{max} = 100L$.

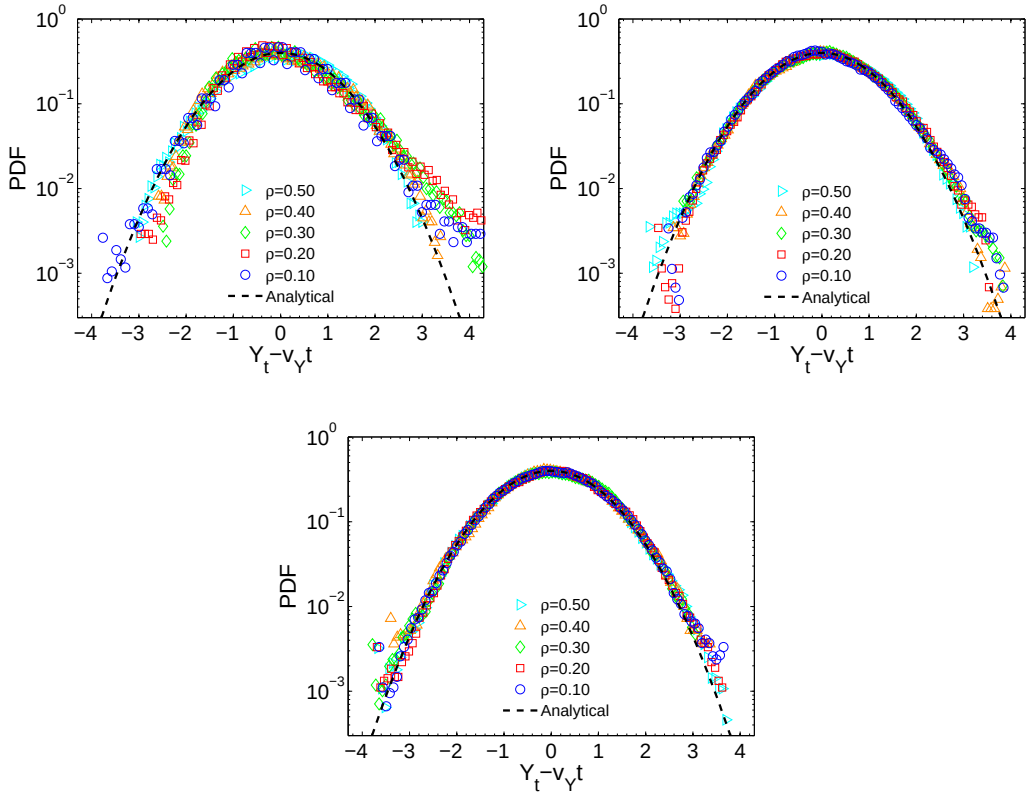

FIG. 10: PDF for Y_t: t= 0.1 L, t= 10 L, t= 100 L. Data points are obtained on a lattice with L=1024; for each value of ρ, simulations for Y_t evolution are repeated 4000 times, each for a time $t_{max} = 100L$.

IV. SPECIAL PARTS

A. Deterministic initial conditions

An important issue is the one related to the link existing between competing surface statistics and the statistics of the overall growing surface. Since the asymptotic shape of the overall growing surface is deterministically related to the particular choice of the initial conditions configurations of particle on the TASEP lattice, we investigate asymptotic speed and fluctuations behaviour for the second class particle and the sector particle using deterministic initial conditions. Deterministic initial conditions correspond to fill one lattice site every $1/\rho$ as follow (for $\rho = 1/3$)

$$..0\,0\,1\,0\,0\,1\,0\,0\,1\,0\,0\,1..\tag{24}$$

Three different choices for ρ are investigated: $\rho = 1/4, 1/3, 1/2$. Comparing numerical speed and fluctuations data obtained for stationary initial conditions with the one obtained using deterministic initial conditions, it turns out that both second class particle and sector particle display the same behaviour (FIGG.11, 12).

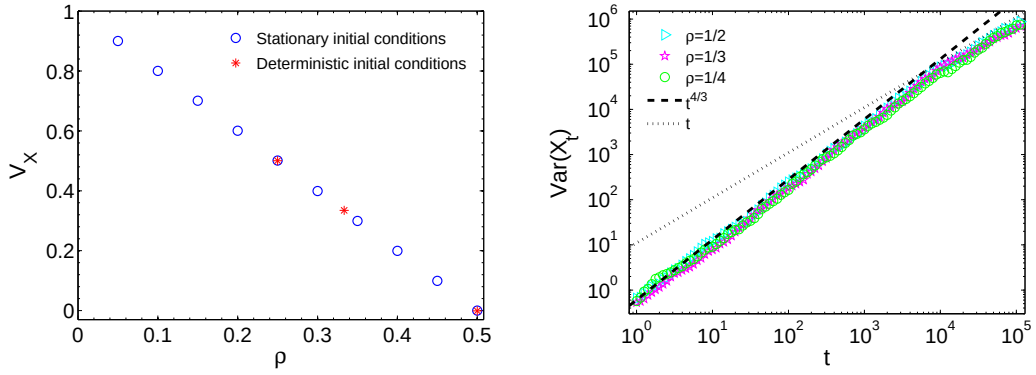

FIG. 11: Asymptotic speed and fluctuations for a second class particle: stationary and deterministic initial conditions. Data points are obtained on a lattice with L=1024; for each value of ρ, simulations for X_t evolution are repeated 4000 times, each for a time $t_{max} = 100L$.

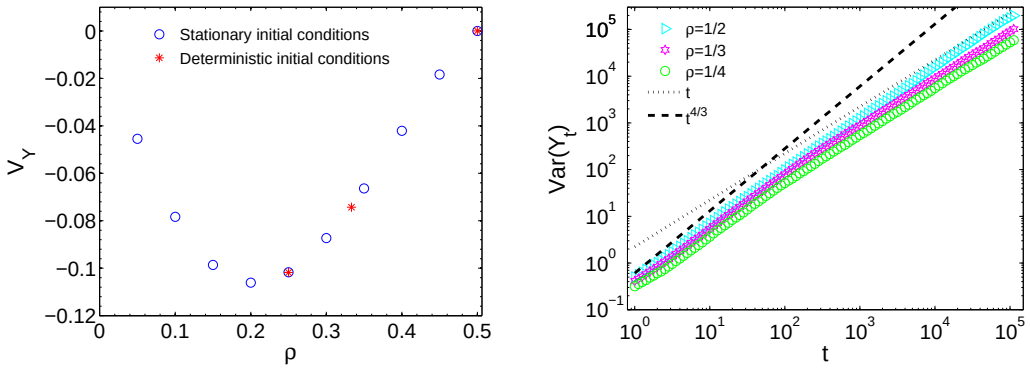

FIG. 12: Asymptotic speed and fluctuations for a sector particle: stationary and deterministic initial conditions. Data points are obtained on a lattice with L=1024; for each value of ρ, simulations for Y_t evolution are repeated 4000 times, each for a time $t_{max} = 100L$.

B. Analysis of Z_t^q

So far we have studied the two extreme inheritance laws that can drive the dynamics of a competing interface between two media: the one corresponding to inheriting the type of the younger parent and related to second class particle in a solid on solid TASEP context, and the one corresponding to inheritate the type of the older parent and modelled by the new sector particle. In this section we present the results obtained for Z_t^q being the interface generated by inheriting the type from the older parent with probability q, and from the younger parent with probability $1 - q$.

In FIG. 13 are displayed asymptotic speeds as functions of ρ for different values of q where $q = 0$ corresponds to the case of sector particle and $q = 1$ to the case of second class particle. Z_t^q interpolates between X_t and Y_t, and for $q = 1/2$ it is easy to see that the interface performs a random walk without drift, i.e. $Z_t/t \to v_Z(\rho) = 0$ for all $\rho \in [0, 1]$.

Fluctuations asymptotic behaviour turns out to be of order t with the same features displayed by a sector particle for $q < 0.5$; to behave like t for all t in the case of $q = 0.5$ since the particle/competing surface is performing a pure brownian motion; to have different asymptotic behaviours (proportional to t or $t^{4/3}$)

depending on ρ for $q > 0.5$. The shrinking phenomenon for fluctuations data points as function of ρ is visible and become more and more accentuated as q approaches 1 meaning a pure second class particle nature.

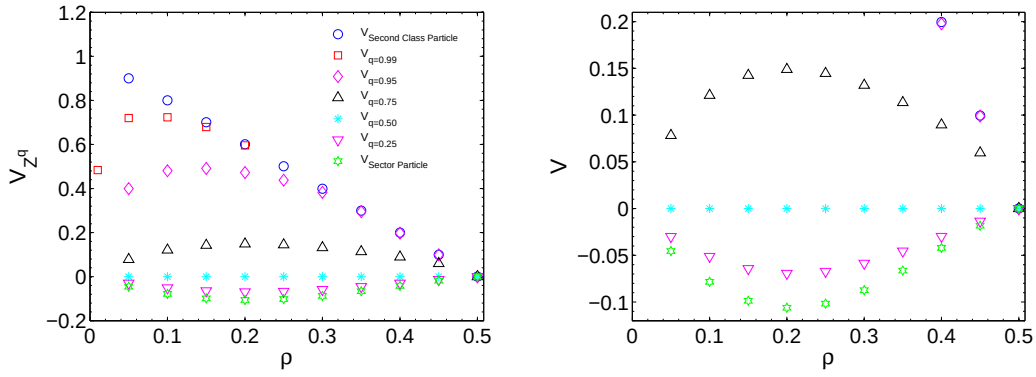

FIG. 13: From second class particle to sector particle: asymptotic speeds (left panel); zoom in of the left panel (right panel). Data points are obtained on a lattice with L=1024; for each value of ρ, simulations for Z_t evolution are repeated 4000 times, each for a time $t_{max} = 100L$.

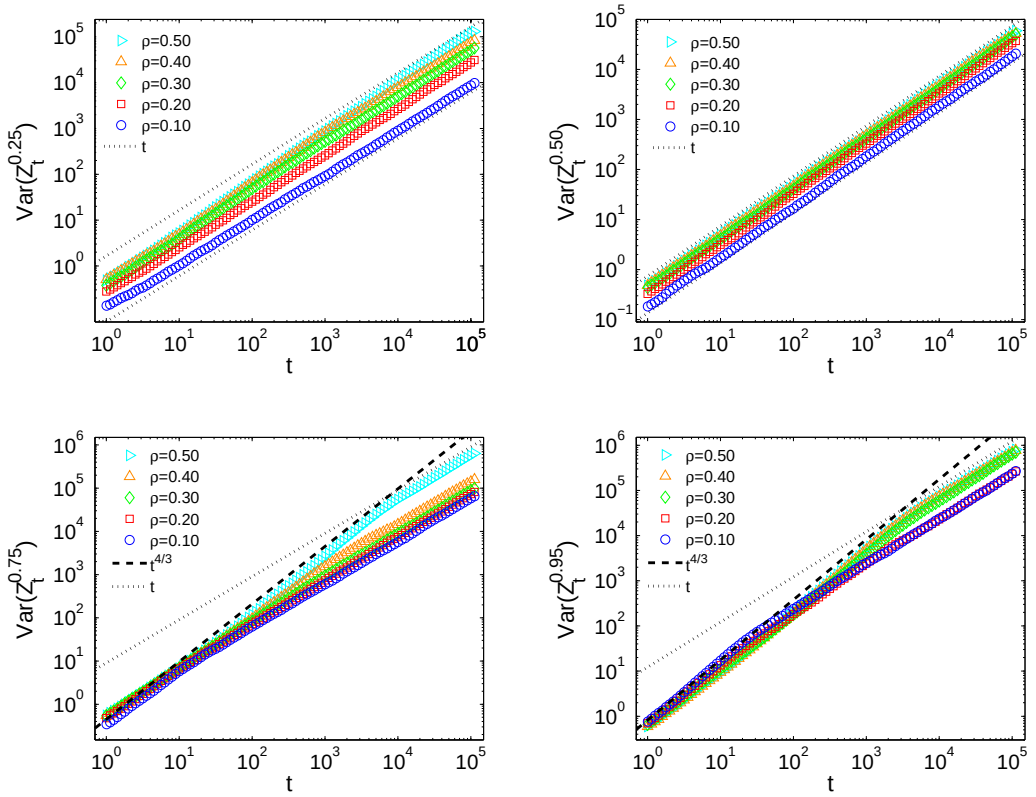

FIG. 14: Fluctuations for several value of q: from top to bottom, left to right $q = 0.25, 0.50, 0.75, 0.95$. Data points are obtained on a lattice with L=1024; for each value of ρ, simulations for Z_t evolution are repeated 4000 times, each for a time $t_{max} = 100L$.

V. CONCLUSION AND PERSPECTIVE

In this work we have done a first attempt to generalize the study of competing surfaces between different media introducing in a solid on solid- TASEP context a new kind of particle different from the well known in literature, second class one. This particle has been draw to mimic the dynamics a competing surface growing according to the law of inheritance by which the new brick inherits the type of the older parent. So far we

investigated numerically the behaviour of asymptotic speed and fluctuations using in particular stationary and deterministic initial conditions. It turned out that sector particle displays an asymptotic speed with a convex functional shape (for ρ ranging from 0 to 0.5), opposite sign respect to second class particle one and non monotonic. Fluctuations do not show the typical behaviour proportional to $t^{4/3}$ displayed instead by second class particle but a diffusive one being asymptotically proportional to t. Superdiffusive (subdiffusive for $\rho = 0.1$ or less) behaviour is displayed for early times. Various attempts to find out analytical results explaining our numerical data have been carried out but they result to be not satisfactory. In the last part of this work the behaviour of particles resulting from the combination of second class and sector particle inheritance laws has also been investigated. This particles turn out to show intermediate features between the one owned by the two extremes second class and sector particle.

A wide range of analytical and numerical perspectives are still open for this work: to find an analytical model explaining the behaviour of the particles introduced; to study the dynamics of this particles using different kind of initial conditions, like cones one.

Acknowledgements

The author is grateful to Stefan Grosskinsky and Adnan Ali for the idea of this project, the support and the interesting discussions and suggestions.

This work has been developed as a M1 project (CSSM - Complex Systems Sciences Master) within Erasmus Mundus program funded by EU.

---

[1] H. Jang, M. J. Grimson, *Thin ferromagnetic films with competing surfaces: A Monte Carlo study of the classical Heisenberg model*, Physical Review B **55**, 1997

[2] I. Rodrguez-Ponce,J. M. Romero-Enrique,L. F. Rull, *Orientational transitions in a nematic liquid crystal confined by competing surfaces*, Physical Review E **64**, 2001

[3] M. Ahr, M. Biehla, *Modelling sublimation and atomic layer epitaxy in the presence of competing surface reconstructions*, Surface Science **488**, 2001

[4] A. Milchev, A. De Virgiliis, K. Binder, *Ising systems with pairwise competing surface fields*, Journal of Physics of Condensed Matter, **17**, 2005

[5] M. Iannuzzi, L. Miglio, *Surface energies and surface relaxation at TiSi2 competing phases*, Surface Science **479**, 2001

[6] I. Goldfarb, P. T. Hayden, J. H. G. Owen, G. A. D. Briggs, *Competing growth mechanisms of Ge/Si001 coherent clusters*, Physical Review B **56**, 1997

[7] O. Hallatschek, P. Hersen, S. Ramanathan, D.R. Nelson, *Genetic drift at expanding frontiers promotes gene segregation*, Proceedings of the National Academy of Science **104**, 2007

[8] A. Ali, S. Grosskinsky, *Pattern formation through genetic drift at expanding population fronts*, Advances in Complex Systems **13**, 2010, arXiv:0912.2241

[9] Y. Saito, H. Müller-Krumbhaar, *Critical Phenomena in Morphology Transitions of Growth Models with Competition*, Physical Review Letters **74**, 1995

[10] M. Kotrla and M. Predota, *Interplay between kinetic roughening and phase ordering*, Europhysics Letters **39**, 1997

[11] B. Derrida, R. Dickman, *On the interface between two growing Eden clusters* ,Journal of Physics A **24**, 1991

[12] N.D. Blair-Stahn, *First passage percolation and competition models*, arXiv:1005.0649

[13] L.P.R. Pimentel, *Multi-type shape theorems for FPP models*, Advances in Applied Probability **39**, 2007

[14] P.A. Ferrari, J.B. Martin, L.P.R. Pimentel, *Roughening and inclination of competition interfaces*, Phys. Rev. E **73**, 2006, arXiv:math/0412198

[15] P.A. Ferrari, L.P.R. Pimentel, *Competition interfaces and second class particles*, Ann. Probab. **33**, 2005

[16] P.A. Ferrari, J.B. Martin, L.P.R. Pimentel, *A phase transition for competition interfaces*, Annals of Applied Probabability **19**, 2009

[17] I.Corwin, *The Kardar-Parisi-Zhang equation and universality class*, arXiv:1106.1596v2

[18] M. Balázs, E. Cator, T. Seppalainen, *Cube root fluctuations for the corner growth model associated to the exclusion process*, Electronic Journal of Probability **11**, 2006

[19] J.B. Martin, *Last-passage percolation with general weight distribution*, Markov Processes and Related Fields **12**,2006, available online at `http://www.stats.ox.ac.uk/~martin/papers.html`

[20] B. Derrida, J.L. Lebowitz, E.R. Speer, *Shock profiles for the partially asymmetric simple exclusion process*, Journal of Statistical Physics **89**, 1997

[21] H. Guiol, T. Mountford, *Questions for second class particles in exclusion processes*, Markov Processes nd Related Fields **12**, 2006

[22] H. Rost, *Nonequilibrium behaviour of a many particle process: density profile and local equilibria*, Probability Theory and Related Fields, **58**, 1981

[23] M. Prähofer and H. Spohn, *Exact scaling functions for one-dimensional stationary KPZ growth*, Physical Review Letters **84**, 2005

[24] T. M. Liggett, *Interacting particle systems*, Springer-Verlag, Berlin (2005)